

# TiO<sub>2</sub>-Zeolite Y Catalyst Prepared Using Impregnation and Ion-Exchange Method for Sonocatalytic Degradation of Amaranth Dye in Aqueous Solution

Atheel Hassan Alwash, Ahmad Zuhairi Abdullah, and Norli Ismail

**Abstract**—Characteristics and sonocatalytic activity of zeolite Y catalysts loaded with TiO<sub>2</sub> using impregnation and ion exchange methods for the degradation of amaranth dye were investigated. The Ion-exchange method was used to encapsulate the TiO<sub>2</sub> into the internal pores of the zeolite while the incorporation of TiO<sub>2</sub> mostly on the external surface of zeolite was carried out using the impregnation method. Different characterization techniques were used to elucidate the physicochemical properties of the produced catalysts. The framework of zeolite Y remained virtually unchanged after the encapsulation of TiO<sub>2</sub> while the crystallinity of zeolite decreased significantly after the incorporation of 15 wt% of TiO<sub>2</sub>. The sonocatalytic activity was enhanced by TiO<sub>2</sub> incorporation with maximum degradation efficiencies of 50% and 68% for the encapsulated titanium and titanium loaded onto the zeolite, respectively after 120min of reaction. Catalysts characteristics and sonocatalytic behaviors were significantly affected by the preparation method and the location of TiO<sub>2</sub> introduced with zeolite structure. Behaviors in the sonocatalytic process were successfully correlated with the characteristics of the catalysts used.

**Keywords**—Sonocatalytic degradation, TiO<sub>2</sub> loaded, ion-exchange, impregnation, amaranth dye, process behavior.

## 1. INTRODUCTION

DEGRADATION of organic pollutants in industrial wastewater has been receiving great research attentions. Titanium dioxide (TiO<sub>2</sub>) is one of the most efficient photocatalysts that have been widely investigated for wastewater treatment due to its low cost, non toxicity, high stability and super hydrophilic properties [1]. However, fast charge carrier recombination and recycling difficulties hold back the success in the usage of bare TiO<sub>2</sub> [2]. Therefore, supporting TiO<sub>2</sub> on different porous materials such as silica [3], carbon [4], clay [5] and zeolite [6] is a plausible solution to eliminate the separation difficulties of ultrafine TiO<sub>2</sub>.

Many important considerations have to be kept in mind when choosing a good support to anchor TiO<sub>2</sub> such as the surface characteristics, stability of the material, hydrophilic/hydrophobic properties, etc. In addition, a good support has

to increase the catalytic activity by enhancing the physical and chemical properties of the modified catalyst [7].

Zeolites are among the most efficient supports for TiO<sub>2</sub> owing to their unique properties such as high surface area, good thermal stability and high absorption towards organic compounds. Furthermore, the presence of acid-base sites in the framework structure of zeolites describes their electron accepting-donating properties [8]. Many successful attempts in the incorporation of TiO<sub>2</sub> either into the internal pores of zeolites or on its external surface to be used in photocatalytic reactions have been reported. Chen et al. [9] and Liu et al. [7] concluded that the immobilization of TiO<sub>2</sub> on zeolites had a positive effect on increasing the activity of the catalysts for photocatalytic degradation of organic compounds in water. However, problems of low penetration, scattering and diffraction of UV light in the solution can reduce the efficiency of the degradation process [10].

Sonocatalytic process is one of the emerging novel technologies in advanced oxidation processes (AOP). It offers the solution to the drawbacks in photocatalytic process owing to the strong penetration ability of ultrasound in water which can usually reach 20–30cm from the energy source [11]. Ultrasonic irradiation has the ability to generate active hydroxyl radicals via pyrolysis of water molecules during the implosion of acoustic cavity bubbles. These radicals are responsible for the degradation of organic pollutants by converting them to smaller harmless molecules [12].

To the best of our knowledge, there is no report dealing with a zeolite-supported TiO<sub>2</sub> catalyst used for sonocatalytic degradation of organic pollutants in water. Therefore, the main objective of this study is to elucidate and correlate the characteristics and catalytic performance of various TiO<sub>2</sub>-incorporated zeolite catalysts. They have been prepared by changing the position of the TiO<sub>2</sub> in the zeolite to be either encapsulated into the internal pores or being deposited on the external surface by changing the catalysts preparation method. The synergistic effects between the heterogeneous catalysts and ultrasonic irradiation have been characterized for degradation of amaranth dye in water. Different characterization techniques such as X-ray diffraction patterns, inductively coupled plasma ICP-MS spectrometer, Fourier transform infrared spectrometry; scanning electron microscopy, transmission electron microscopy and AFM technique have been used to elucidate the physical and chemical properties of the catalysts to be subsequently correlated with their sonocatalytic activity.

Atheel Hassan Alwash is with the School of Chemical Engineering, Universiti Sains Malaysia, Department of Chemistry, College of Science, Al-Nahrain University, Al-Jadiriya, Baghdad, Iraq (Tel: 0060174593438, e-mail: atheel\_eng78@yahoo.com).

Ahmad Zuhairi Abdullah is with the School of Chemical Engineering, Universiti Sains Malaysia.

Norli Ismail is with the School of Industrial Technology, Universiti Sains Malaysia.

### A. Materials

H-Y zeolite with a Si/Al ratio of 15 was obtained from Zeolyst International. Amaranth dye (see Fig. 1), potassium titanoxalate dehydrate (99%) and sodium chloride bioxtra (99.5%) were obtained from Sigma-Aldrich. Distilled deionized water was obtained by purifying distilled water with an Elga-Pure Water Purification (UHQ W) system.

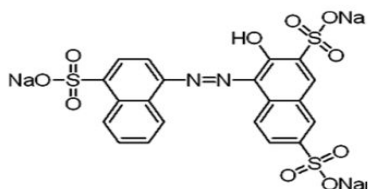


Fig. 1 Chemical Structure of amaranth dye

### III. CATALYST PREPARATION METHOD

#### A. Preparation of Na-Y Zeolite

The dried H-Y zeolite was first converted to its sodium form by means of an ion exchange method [13]. The material was first treated with 1M of NaCl at 80°C for 4h in such a way that the ratio of zeolite Y to sodium chloride solution was 1:80. The slurry was then filtered and washed with distilled deionized water to remove excess NaCl. In order to achieve complete exchange of sodium into the zeolite, the procedure was repeated twice. The sample was then dried over night at a temperature of 80°C and then calcined in a muffle furnace at 550°C for 5h.

#### B. Encapsulation of TiO<sub>2</sub> into Na-Y Zeolite through Ion Exchange Method

Different concentrations of TiO<sub>2</sub> encapsulated into NaY were achieved using the procedure as reported by Liu et al. [7]. Known amounts of potassium titanoxalate were first dissolved in 100mL of distilled deionized water. Then, 1.0g of support (Na-Y zeolite) was added to each solution and the mixtures were kept under continuous stirring for 12h at ambient temperature to allow ion-exchange process. After the ion-exchange step, the solid samples were washed with excessive amount of water. Then, they were dried overnight in an oven at 100°C. The above procedure was repeated twice to get a higher loading of titanium and the corresponding catalysts are denoted as Ti<sub>1</sub>-NaY, Ti<sub>2</sub>-NaY, Ti<sub>3</sub>-NaY, and Ti<sub>4</sub>-NaY according to increasing titanium content in catalyst. Next, the catalysts were calcined in a furnace at 550°C for 5h with a ramping rate of 5°C/min.

#### C. Loading of TiO<sub>2</sub> onto NaY through Impregnation Method

Loading of TiO<sub>2</sub> onto the surface of zeolite from 5-20wt.% TiO<sub>2</sub> (theoretical proportion of TiO<sub>2</sub> in the catalyst) was achieved by means of a wet impregnation method. Different amounts of titanoxalate precursor were dissolved in water and mixed with 1g of NaY for 24h at ambient temperature. Then, the liquid was evaporated in a rotary evaporator and the produced solids were dried in an oven at 120°C for 4h. After the drying process, the catalysts were calcined at 550°C for 5h.

Physicochemical characterizations of the catalysts with different analytical techniques were performed on the most potential catalysts. The amount of titanium incorporated into NaY after the ion-exchange process was determined by means of an inductively coupled plasma ICP-MS spectrometer. Meanwhile, X-ray diffraction patterns of the catalyst samples were obtained using an XRD system (Philips Goniometry PW 1820). The reflectance spectra of solid samples were determined using UV-vis spectrophotometer (PerkinElmer) in a wavelength range from 190 to 1100nm. The surface morphology of the catalyst was investigated using a scanning electron microscope (SEM) unit (Oxford INCA/ENERGY-350) equipped with an energy dispersive X-ray analysis (EDAX) system. In addition, FT-IR spectroscopic measurement was carried out using a Perkin-Elmer spectrophotometer in which the spectra were recorded in the range of 400-4,000 cm<sup>-1</sup>. Transmission electron microscope (TEM) images were obtained using a Phillips CM 12 transmission electron microscope equipped with an image analyzer and operated at 120kV, while the roughness of the catalyst surface was investigated using SPA 400 atomic force microscopy (AFM) technique.

### V. SONOCATALYTIC REACTION

An ultrasonic bath (Cole-Parmer) with an output power of 50W and a frequency of 40kHz was used for all the experimental runs. The reaction dye solution was first stirred for 30min prior to the ultrasonic reaction to maintain good dispersion of catalyst with the dye solution. The experimental conditions were set at an initial amaranth dye concentration of 10mg/L, a catalyst amount of 1.5g/L while the solution pH was kept at its original level without any adjustment. The decolorization efficiency of amaranth dye was calculated based on absorbance recorded using a UV-vis spectrophotometer. During the reaction, 7mL of the solution was withdrawn at each time interval and centrifuged using a Kubota 5910 centrifuge to separate the supernatant. Then, the concentration of the dye solution was determined at a maximum absorbance wavelength of 521 nm. The decolorization efficiency of the catalyst was calculated based to the following equation;

$$\text{Decolorization efficiency (\%)} = [1 - C_t/C_0] \times 100 \%$$

where, C<sub>0</sub> (mg/L) is the initial concentration of dye and C<sub>t</sub> (mg/L) is the concentration of dye at certain reaction time, t (min).

### VI. SURFACE HYDROPHILIC TEST

The surface hydrophilicity measurement was also carried out on the catalysts (NaY, Ti<sub>4</sub>-NaY and 15%TiO<sub>2</sub>-NaY) similar to the procedure reported by Reddy et al. [14] in order to investigate changes in the hydrophilic/hydrophobic properties after the introduction of the TiO<sub>2</sub>. A mixture solution of 0.003M concentration was prepared using salicylic acid (a polar compound) and a non-polar solvent (hexane). Then, 2g/L of the catalyst was added into the solution under continuous stirring for 2h. The liquid

samples were then taken at each time interval and centrifuged to remove the catalyst. Then, UV-VIS spectrophotometer measurement was performed at  $\lambda_{\max}$  312nm to determine the residual concentration of salicylic acid in the solution.

## VII. RESULT AND DISCUSSION

### A. X-Ray Diffraction (XRD)

The XRD diffraction patterns for parent zeolite (NaY), potassium titanio oxalate after calcination at 550°C for 5h ( $\text{TiO}_2$ ),  $\text{TiO}_2$  encapsulated zeolite ( $\text{Ti}_4\text{-NaY}$ ) and  $\text{TiO}_2$  loaded through impregnation on the surface of zeolite (15%  $\text{TiO}_2\text{-NaY}$ ) are shown in Fig. 2. It is clear that Na-Y zeolite had an excellent crystallinity based on its sharp peak and high intensities. Tayade et al. [13] reported the reflections of NaY at  $2\theta$  values of 12°, 15°, 18°, 20°, 23°, 31°, and 34° which were in agreement with our results. The structure of  $\text{Ti}_4\text{-NaY}$  has no different as compared to that of NaY and no new peaks for anatase phase was detected. This was ascribed to the low amount of titanium being exchanged into the zeolite as it was verified by ICP analysis (0.3 wt.% Ti). Due to the fact that usually, the surface area of zeolites is contributed by the internal pores, the ion-exchange process should be theoretically dominant there. It was also possible that the clusters of the  $\text{TiO}_2$  formed after the calcination step was very small to give any clear diffraction patterns. However, there were small reductions in the peaks intensity of the  $\text{Ti}_4\text{-NaY}$  after the encapsulation of  $\text{TiO}_2$ . Chen et al. [9] did not detect any peak for titanium oxide encapsulated into zeolite below 83mg/g of catalyst. However, when the impregnation method was used for the incorporation of  $\text{TiO}_2$  on the surface of zeolite, the crystallinity of the zeolite significantly disappeared and the structure was converted to amorphous with wide rutile peak at  $2\theta$  value of 27.7°.

It was well reported in literatures that the transformation phase temperatures for the case of 15%  $\text{TiO}_2\text{-NaY}$  from anatase to rutile are usually occurred between 700-800°C [15], [16]. However, the calcination temperature used in this study was 550°C. Therefore, the high calcination temperature used during the preparation method was not suggested to be the reason behind the appearance of the rutile phase. Instead, the type of the precursor used in this study was deemed responsible for accelerated the formation of rutile phase. Accordingly, the effect of titanium precursor on the crystallinity of zeolite was investigated using impregnation method by changing the potassium titanium oxalate source used in this study with another organic liquid precursor i.e. tetra butyl orthotitanate (TBT) and the catalyst was denoted as 15% TBT-NaY as shown in Fig. 2. The results indicated that zeolite support was able to retain its high crystallinity after the loading of  $\text{TiO}_2$  with a significant reduction in the main high peaks intensities of zeolite after the loading of  $\text{TiO}_2$ . Furthermore, a small anatase peak was detected after the loading of 15% TBT into NaY. As a result, it seemed that the dispersion of  $\text{TiO}_2$  clusters onto zeolite depend on the type of titanium precursor used and its action during the preparation method. From Fig. 2, it is also noted that the unsupported  $\text{TiO}_2$  had an amorphous structure without any anatase peak at  $2\theta$  of 25.1° which is well known to be the most significant peak in anatase phase.

From Fig. 2, only small peak was detected for anatase phase at  $2\theta$  value 48.1° and it disappeared after the  $\text{TiO}_2$  loading on the zeolite. As a result, it can be concluded that the type of precursor as a starting material had a significant effect on the formation of the  $\text{TiO}_2$  phase. Similarly, Durgakumari et al. [17] concluded that the formation of  $\text{TiO}_2$  phase in H-ZSM-5 was affected by the type of precursor used.

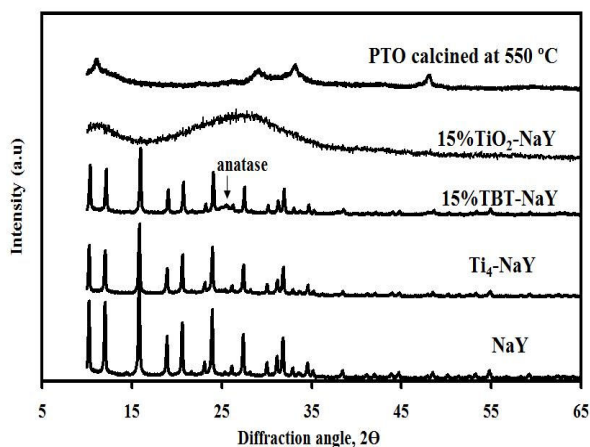


Fig. 2 X-ray diffraction patterns for parent NaY,  $\text{Ti}_4\text{-NaY}$  prepared using an ion-exchange method and 15%  $\text{TiO}_2\text{-NaY}$  prepared using an impregnation method

The average crystallite size for NaY,  $\text{Ti}_4\text{-NaY}$  and 15%  $\text{TiO}_2\text{-NaY}$  samples were calculated using the Scherrer equation based on the highest peaks for each catalyst in Fig. 2. NaY and  $\text{Ti}_4\text{-NaY}$  showed high crystalline structure with average crystallite sizes of 60.2nm and 49.6nm. However, the average crystallite size in the case of 15%  $\text{TiO}_2\text{-NaY}$  catalyst was ascribed to the rutile peak only that was detected after the loading of 15%  $\text{TiO}_2$ . The average crystalline size was significantly reduced in the case of 15%  $\text{TiO}_2\text{-NaY}$  catalyst to (1.78nm) which was considerably larger than the pore size and super cage of zeolite i.e. 0.74 nm and 1.3nm, respectively. The wide and low intensity peak for this catalyst gave an indication to the small crystalline size which was ascribed to the rutile phase that accumulated on the surface of zeolite [18]. Partial interaction between Ti species and zeolite framework could also occur during impregnation method (15%  $\text{TiO}_2\text{-NaY}$ ) since the same titanium precursor was used. Consequently, the excess amount of Ti species could be anchored on the surface of the support after the calcination step lead to a significant reduction in the crystallinity and the average crystal size of the 15%  $\text{TiO}_2\text{-NaY}$  catalyst.

### B. Diffuse Reflectance Spectra

The UV-vis reflection spectra was carried out for the parent NaY, encapsulated  $\text{TiO}_2$ , 15%  $\text{TiO}_2\text{-NaY}$  and the bare PTO (potassium titanium oxalate) calcined at 550°C as reference is shown in Fig. 3. Blue shifts towards shorter wave lengths at 372nm were observed for encapsulated titanium ( $\text{Ti}_4\text{-NaY}$ ) while the bare  $\text{TiO}_2$  had a wave length of about 390 nm. This behavior was in agreement with Easwaramoorthi and Natarajan [19]. The sudden fall in the reflectance at certain wave lengths indicated the presence of optical band gap due to the encapsulation of Ti species into

the framework of zeolite after the ion-exchange process [10]. The provenance of such blue shift towards shorter wave length was due to the quantum size effect for semiconductors as the particle size decreased after the modification of  $\text{TiO}_2$  into the pores of the zeolite. The phenomenon of size quantization is expressed in terms of reduction in particles size of  $\text{TiO}_2$  into nano-scale clusters. Thus, more light would be absorbed at very short wavelength light with energy larger than the band gap energy of semiconductors thus facilitate the electronic excitation of  $\text{TiO}_2$  catalyst [21].

On the other hand, for the case of 15%  $\text{TiO}_2$ -NaY, there was a slight decrease in the reflectance spectra of 15%  $\text{TiO}_2$ -NaY at wave length of 390nm in comparative to that of potassium titanium oxalate (PTO) calcined at 550°C. However, no significant red or blue shifts were detected for the catalyst with respect to the bare PTO calcined at 550°C. This similarity of reflectance spectra between 15%  $\text{TiO}_2$ -NaY and the unsupported PTO was ascribed to the dispersiveness of  $\text{TiO}_2$  with the top layer of zeolite that causes the blockage of the pore surface of zeolite and the accumulation of the excess amount of  $\text{TiO}_2$  on the external surface of zeolite thus shortening the diffusion length into zeolite framework. As a result, it can be concluded that the preparation method can affect the diffusion rate between the active component and support thus, influence the optical properties of the produced catalyst.

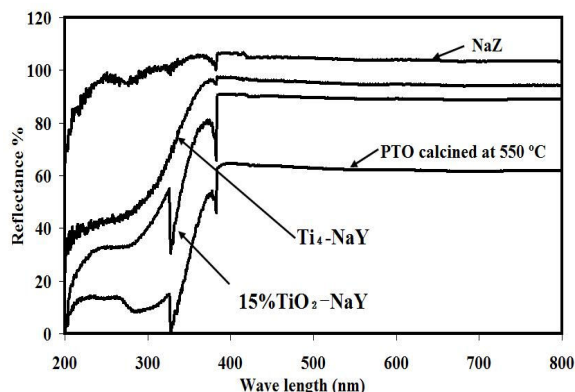


Fig. 3 The UV-Vis diffuse reflectance spectra for different types of catalysts

#### C. FT-IR Spectroscopic Measurement

Fig. 4 shows the FTIR spectra for NaY,  $\text{Ti}_4$ -NaY and 15%  $\text{TiO}_2$ -NaY samples. The strongest peak at around  $1,067\text{cm}^{-1}$  for all the samples is assigned to the framework stretching vibration band of O-T-O or T-O-T (where T represents to Al or Si atom) [18]. For the case of the encapsulated  $\text{TiO}_2$ , evidence of partial replacement of Ti with Si was detected after the preparation procedure as a characteristic peak at  $960\text{cm}^{-1}$  was detected. Petkowicz et al. [6] assigned this peak to the anti symmetric stretching vibration of the Ti-O-Si band. However after  $\text{TiO}_2$  loading using impregnation method, no such peak could be detected. Therefore, the dispersion of  $\text{TiO}_2$  was suggested to mainly occur on the external surface of the zeolite and could partially incorporate into the top layers of zeolite [16].

For both cases of  $\text{Ti}_4$ -NaY and 15%  $\text{TiO}_2$ -NaY, a stretching vibration observed between 500 and  $700\text{cm}^{-1}$

was attributed to the sensitive change in the pseudo-lattice vibration of zeolite after the loading of  $\text{TiO}_2$  [22]. Meanwhile, bands below  $400\text{cm}^{-1}$  were ascribed to lattice vibrations. However, a stretching vibration peak attributed to Ti-O bond was also observed at  $460\text{cm}^{-1}$ . Therefore, it can be concluded that the usage of different preparation methods could affect the nature of interaction between  $\text{TiO}_2$  with the framework elements of the zeolite. In this respect, ion-exchange method involves chemical interaction while impregnation method only involves physical interaction.

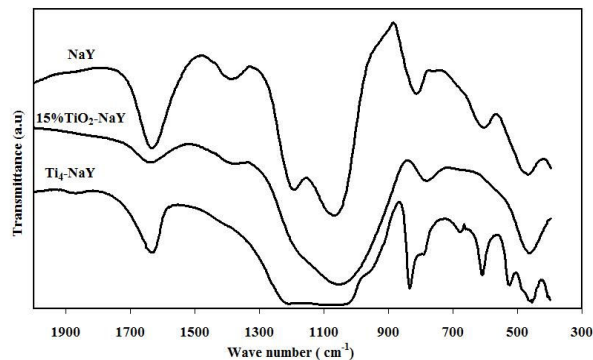


Fig. 4 FTIR spectra for parent for different samples

#### D. Scanning Electron Microscopy and EDAX Technique

Surface morphology of NaY,  $\text{Ti}_4$ -NaY and 15 %  $\text{TiO}_2$ -NaY samples are shown in Fig. 5. The NaY presented a polyhedral crystalline structure as in Fig. 5 (a) and the crystal structure of the zeolite was visibly preserved after the loading of  $\text{TiO}_2$  for both cases (encapsulated or loaded on the external surface of zeolite). Meanwhile, the smoothness of the catalyst surface did not reveal any visible difference comparing to NaY as in Fig. 5 (b) and (c). The presence of  $\text{TiO}_2$  clusters were also recorded to be not clearly observed by the work of Yamaguchi et al. [23] for 25 wt.%  $\text{TiO}_2$  loaded on H-MFI. Furthermore, this result proved that the loading of  $\text{TiO}_2$  did not pose significant damage to the crystalline structure of zeolite which came with a good consistent with the XRD results. The disappearance of the high intensity peaks characteristics of zeolite was mainly ascribed to the  $\text{TiO}_2$  phase evenly accumulated on the surface.



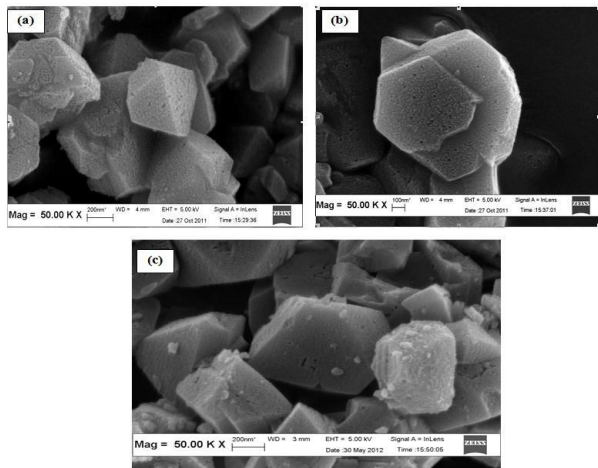


Fig. 5 Surface morphology of (a) NaY, (b)  $\text{Ti}_4\text{-NaY}$  and, (c) 15 %  $\text{TiO}_2\text{-NaY}$

The EDAX technique was used to analyze the surface elemental composition of the solid support and catalysts. Fig. 6 (a) indicated the presence of Ti species on the surface of the zeolite for the case of 15%  $\text{TiO}_2\text{-NaY}$  prepared using impregnation method. Inversely, for the case of the ion-exchanged method, no Ti was detected on the surface of  $\text{Ti}_4\text{-NaY}$  catalyst. Instead of that, it was mainly deposited on the internal surface as suggested by the result in Fig. 6 (b). These results suggested the successful encapsulation of  $\text{TiO}_2$  into the super cages or the channels of zeolite. In similar work, Easwaramoorthi et al. [24] also did not detect any Ti element on surface of zeolite Y and concluded that the presence of  $\text{TiO}_2$  nano clusters was mainly located in the cages of zeolite.

#### E. Transmission Electron Microscope

The TEM imaging was carried out for parent NaY,  $\text{Ti}_4\text{-NaY}$  and 15 wt%  $\text{TiO}_2\text{-NaY}$  catalysts. The unmodified zeolite structure can be observed in Fig. 7 (a), (b) for two different magnifications i.e. 8kX and 45kX, respectively. The hexagonal crystalline geometry of the zeolite remained virtually unchanged after the loading of 15 wt% of  $\text{TiO}_2$  using impregnation method as was observed in Fig. 7 (c).

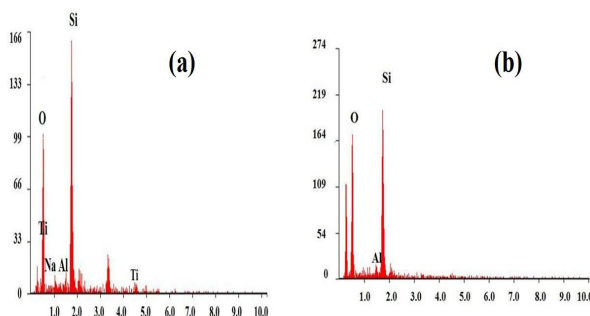


Fig. 6 EDAX results for (a) 15 %  $\text{TiO}_2\text{-NaY}$  and, (b)  $\text{Ti}_4\text{-NaY}$

This results as well as results of the SEM/EDAX analyses proved that the zeolite was generally able to maintain its original structure after the loading of 15 wt% of  $\text{TiO}_2$  since no significant damages were detected on the its hexagonal structure. Furthermore, the TEM results suggested that the position of  $\text{TiO}_2$  clusters were mainly positioned on the

surface of zeolite due to appearance of many white clusters accumulated on the hexagonal zeolite structure. Inversely, for the case of encapsulated  $\text{TiO}_2$  ( $\text{Ti}_4\text{-NaY}$ ) a significant black dots ascribed to  $\text{TiO}_2$  clusters were detected as in Fig. 7 (d) due to the position of these clusters inside the cages of zeolite (shielded by zeolite structure as Ti is a heavier element than Si or Al). Similar results have been reported by Bossmann et al. [18] for Ru/ $\text{TiO}_2$  - doped zeolite Y. The reason behind the appearance of black and white clusters of  $\text{TiO}_2$  for both catalysts was ascribed to the difference in  $\text{TiO}_2$  position and the amount of  $\text{TiO}_2$  loading. However, it was difficult to determine the accurate size of  $\text{TiO}_2$  due to the overlapping metals crystallites within the zeolite matrix.

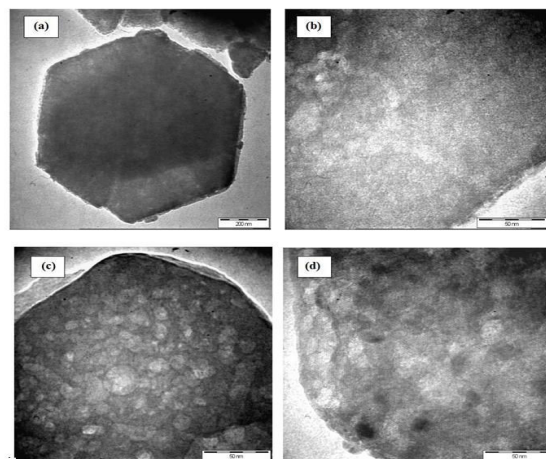


Fig. 7 TEM images for (a and b) NaY, (c) 15 %  $\text{TiO}_2\text{-NaY}$  and, (d)  $\text{Ti}_4\text{-NaY}$

#### F. Atomic Force Microscopy / AFM technique

The surface uniformity of the parent NaY,  $\text{Ti}_4\text{-NaY}$  and 15% $\text{TiO}_2\text{-NaY}$  were analyzed using an AFM technique. Fig. 8 shows the in the three dimensional (3D) and two dimensional (2D) AFM images for all types of catalysts. The results suggested that the degree of roughness was in the sequence of NaY and  $\text{Ti}_4\text{-NaY}$  > 15 % $\text{TiO}_2\text{-NaY}$  with roughness values of 72 - 74nm and 44nm, respectively. In Fig. 8 image (a), (b), both NaY and  $\text{Ti}_4\text{-NaY}$  surfaces had approximately the same roughness value around 72-74nm. This similarity in the roughness of the catalyst surfaces before and after the loading of titanium was attributed to the absence of  $\text{TiO}_2$  from the surface of the catalyst. Instead, it was mainly encapsulated into the pores of the zeolite. However, it was clear that the roughness of the catalyst decreased drastically after the loading of  $\text{TiO}_2$  for 15%  $\text{TiO}_2\text{-NaY}$  due to the small crystal size of the supported  $\text{TiO}_2$  which was in agreement with XRD results. It is clear in Fig. 8 that surface morphology of 15%  $\text{TiO}_2\text{-NaY}$  seemed to be like a layer covered the surface due to the accumulation of  $\text{TiO}_2$  on the zeolite. These results have been approved also by the EDX, XRD and UV-vis results as discussed in earlier sections.

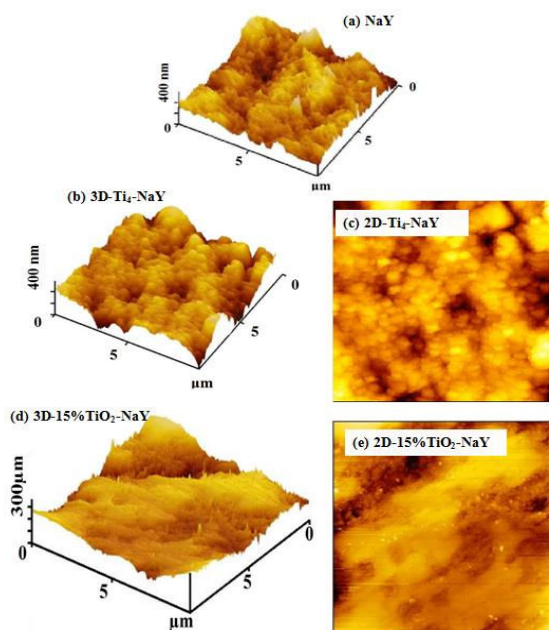


Fig. 8 Two and three dimension AFM images for NaY,  $\text{Ti}_4\text{-NaY}$  and  $15\%\text{TiO}_2\text{-NaY}$

## VIII. SONOCATALYTIC DEGRADATION PROCESS

### A. Control Experiment

Before further investigation on the sonocatalytic performance of various heterogeneous catalysts, preliminary experiments were carried out to assess the role of catalyst under ultrasonic reaction and the results were presented in Fig. 9. A silent experiment study without the presence of ultrasonic irradiation was carried out to check the absorption of amaranth dye under continuous stirring for 120min by both types of  $\text{TiO}_2$  loaded zeolite. The experimental runs were carried out at an initial dye concentration of  $10\text{mg/L}$ , a catalyst loading of  $1.5\text{g/L}$  and its natural pH. No significant variation in the concentration of the amaranth dye was observed during the continuous stirring process. The decolorization efficiency under ultrasonic irradiation without the presence of catalyst was also investigated under the same reaction condition and the decolorization efficiency was only about 12%. This low efficiency of the process could be ascribed to the insufficient amount of generated hydroxyl radicals ( $\bullet\text{OH}$ ) which are considered the main active species involved in the dye degradation process. The activity of these radicals could be affected by the ultrasonic power, as well as the size and the chemical structure of the dye molecules concerned in the reaction. The presence of solid catalyst in conjunction effect with ultrasonic irradiation was able to increase the removal efficiency to 45%, 50%, and 68% for calcined PTO (potassium titanium oxalate),  $\text{Ti}_4\text{-NaY}$  and  $15\%\text{TiO}_2\text{-NaY}$ , respectively. This increases suggested the differences in the sonocatalytic performance of the catalysts. The efficiency of  $15\%\text{TiO}_2\text{-NaY}$  catalyst was the most active catalyst in comparative to the encapsulated titanium  $\text{Ti}_4\text{-NaY}$  due to the difference in  $\text{TiO}_2$  content within zeolite structure. Furthermore, the presence of heterogeneous solids could enhance trapping the vapor gas nuclei through the pores causing an increase in the generation of free radicals [15].

I:7, No:

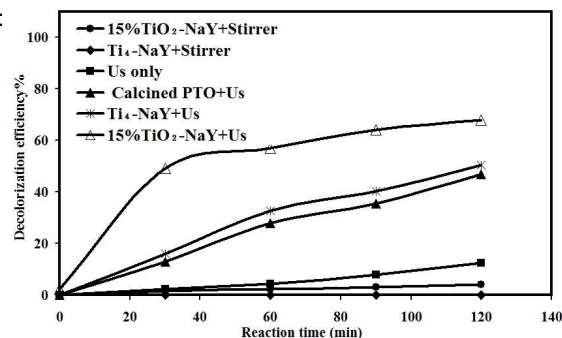


Fig. 9 Preliminary experimental runs with and without ultrasonic irradiation ( $10\text{mg/L}$  initial dye concentration,  $1.5\text{g/L}$  catalyst loading, original pH and 120min of reaction)

### B. Effect of $\text{TiO}_2$ loading

The behaviors of the sonocatalytic degradation of amaranth dye in the presence of zeolite catalyst with different loadings of  $\text{TiO}_2$  either encapsulated into zeolite or incorporated at zeolite surface were shown in Fig. 10. The sonocatalytic reaction was performed under the same reaction conditions. Sonocatalytic activity was clearly enhanced by increasing the loading of  $\text{TiO}_2$  into the pores of the zeolite. The highest decolorization efficiencies achieved in 120min were found to be increased reaching its maximum decolorization of 50.3% for  $\text{Ti}_4\text{-NaY}$ . The enhancement in the decolorization efficiency of amaranth was associated with the formation of more hydroxyl radicals generated by the encapsulated titanium oxide with increasing  $\text{TiO}_2$  loading.

Increasing the level of active component could lead to the generation of more hydroxyl radicals which were responsible for the oxidation of the dye molecules [11]. In this case, the role of pore diffusion limitation at high  $\text{TiO}_2$  loadings was not significant. In addition, zeolite also played an important role in inhibiting the  $\text{e}^- \cdot \text{h}^+$  recombination when irradiated with ultrasound due to its amphoteric properties in accepting-donating electrons. High surface area and the hydrophilic/hydrophobic properties allowed the zeolite framework to absorb different intermediate products during the reaction. Meanwhile,  $\text{TiO}_2$  is known to be a super hydrophilic material so the affinity towards adsorption of hydrophobic materials is low [8]. So the energy generated by the ultrasound was not shielded by the adsorbed species on the surface.

The enhancement in sonocatalytic reaction should also be referring to the advantages of ultrasonic irradiation in providing mechanical stirring effects that offers the mixing between the generated hydroxyl radicals and dye molecules. It is also served for continuous cleaning of the catalyst surface due to the mechanical effects post by water jets. According to results presented in Fig. 10, the ultrasonic wave was able to reach the internal pores of the zeolite throughout the reaction medium as the titanium clusters were located there. Therefore, it was suggested that these clusters were located closer to the external surface of the zeolite with increasing loading of  $\text{TiO}_2$ . Thus, the decolorizing efficiency was improved by the intensified generation of free radicals by higher amounts of encapsulated  $\text{TiO}_2$  as well as the improved mass transfer within the internal pores [11].

Effects of different preparation methods of  $\text{TiO}_2$ -loaded zeolite Y in the sonocatalytic degradation of amaranth can be characterized based on results in Fig. 10. The Effect of  $\text{TiO}_2$  loading on zeolite through impregnation method from 5-20 wt% of  $\text{TiO}_2$  loading was investigated and the decolorization efficiency was found to increase from 54.5% to 68% by increasing the loading from 5 to 15 wt%. However, the sonocatalytic efficiency of amaranth slightly decreased to 59% with further increase in the  $\text{TiO}_2$  loading to 20 wt%. It was observed that there was an optimum amount for the loading of  $\text{TiO}_2$  into the zeolite. Below the optimum level, the generation of the radicals was not significantly high for degradation of the dye molecules so that increasing of active sites led to an increasing in the removal efficiency.

As the amount of  $\text{TiO}_2$  was further increased beyond 15 wt%, excessive  $\text{TiO}_2$  deposition on the pore mouths could clog some of the pores. Thus, the reduction in the activity of zeolite catalyst for 20 wt%  $\text{TiO}_2$  loading could be ascribed to multiple reasons such as the increase in the aggregation of  $\text{TiO}_2$  clusters on the surface of the NaY with the increase in of  $\text{TiO}_2$  amount incorporated [16]. Furthermore, according to AFM results for the case of 15%  $\text{TiO}_2$ -NaY, the  $\text{TiO}_2$  formed a layer cover the surface of zeolite. Subsequently, increasing the loading of  $\text{TiO}_2$  will increase the thickness of the layer thus reduce the diffusion rate between  $\text{TiO}_2$  and zeolite surface. This would increase the probability for  $e^-h^+$  recombination when some particles of titanium oxide underwent separation from zeolite and aggregation [25].

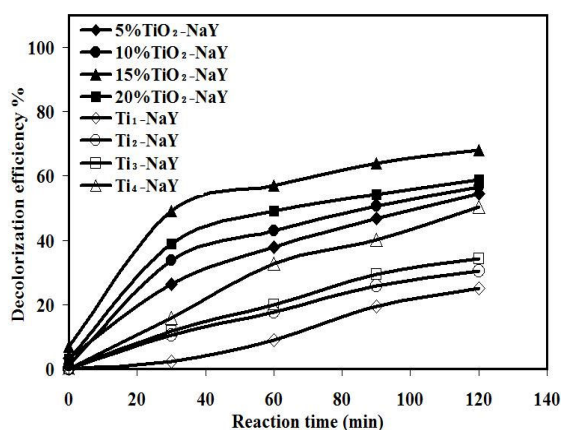


Fig. 10 Degradation efficiency of amaranth dye with different loadings of  $\text{TiO}_2$  encapsulated or being loaded onto zeolite (10mg/L initial dye concentration, 1.5g/L catalyst loading, and original pH)

From these results, it was clear that the preparation method played a significant role in influencing of the characteristics of the catalyst as well as their sonocatalytic behaviors. For the case of encapsulated titania, the amount of Ti species inside the pores of zeolite was considered small due to the low exchange capacity of the zeolite (high Si/Al ratio). While for the case of impregnation method (15%  $\text{TiO}_2$ -NaY) the partial interaction with zeolite could be occurred and the excess amount of  $\text{TiO}_2$  was anchored on the external surface of the support. Therefore, the difference in  $\text{TiO}_2$  loading for the produced catalysts after the preparation method had an effect on the sonocatalytic

behavior. Furthermore, the position of  $\text{TiO}_2$  i.e. either within the internal pores of zeolite or being loaded at its external surface of it had a significant effect on the sonocatalytic behavior. This was because the ultrasonic wave could easily activate the  $\text{TiO}_2$  clusters loaded on the external surface of zeolite comparing to the encapsulated  $\text{TiO}_2$  into the internal pores due to the direct of contact between the ultrasonic wave and the active component. Furthermore, the rate of internal diffusion could also affect the overall performance of the catalyst. As a result,  $\text{TiO}_2$  loading on the external surface of zeolite showed higher catalytic activity.

#### IX. THE HYDROPHILIC/HYDROPHOBIC PROPERTIES OF THE SYNTHESIZED CATALYST

Hydrophilic/hydrophobic property is an important factor that can affect on the ability of the catalyst to absorb a great variety of organic compounds. One of the most important factors that can change this property in zeolites to be either hydrophobic or hydrophilic is their Si/Al ratio. In general, the higher the ratio, the more the hydrophobicity of zeolite is. However, it can also be influenced by other factors such as the type and concentration of the doping materials [12]. It is of great interest to investigate the hydrophilic / hydrophobic characteristics of the parent NaY,  $\text{Ti}_4$ -NaY and 15%  $\text{TiO}_2$ -NaY prepared using ion-exchange and impregnation method, respectively. The ability of the catalyst to absorb polar or non-polar compounds can give an indication about the nature of these materials to be either hydrophilic or hydrophobic materials.

It can be concluded in Fig. 11 that  $\text{TiO}_2$  had a rather hydrophilic property and reached its equilibrium state after about 30 min due to the rapid absorption of salicylic acid. Meanwhile, NaY showed rather more hydrophobic property compared to other catalysts. Thus, the low ability of NaY to absorb the salicylic acid was ascribed to its high Si/Al ratio of 15 (low Al content). However, after the loading of  $\text{TiO}_2$  into the NaY, the hydrophilicity increased and obviously influenced by the loading of  $\text{TiO}_2$  in the zeolite. From ICP analysis, the amount of Ti encapsulated in the zeolite was measured to be only 0.3 wt%. Therefore, the difference in hydrophilicity of encapsulated titanium  $\text{Ti}_4$ -NaY was very small compared with that of the parent NaY. In case of 15%  $\text{TiO}_2$ -NaY, the catalyst was more hydrophilic due to the higher concentration of  $\text{TiO}_2$  anchored on its surface. Higher hydrophilicity allowed more adsorption of dye molecules to interact with the  $\text{TiO}_2$  clusters in the zeolites. As the hydroxyl radicals were also generated on the surface of the  $\text{TiO}_2$  nanoparticles, better interaction between them would facilitate the degradation process.



The Research University grant from Universiti Sains Malaysia to support this work is gratefully acknowledged.

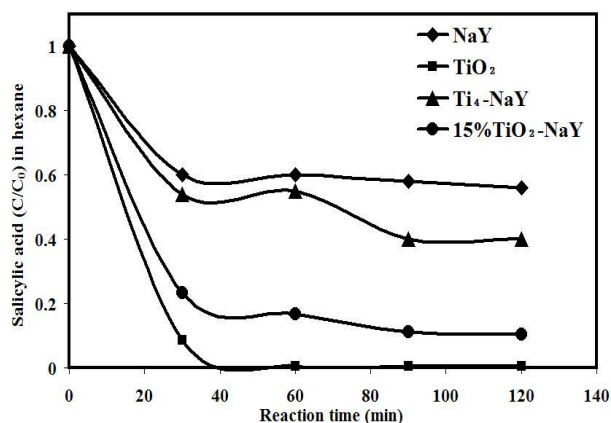


Fig. 11 Effect of hydrophilic/hydrophobic properties of the catalysts on the adsorption of salicylic acid in hexane

The absorption capacity of zeolite during the reaction is generally affected by the nature of the cations that presents in its own framework [26]. Serralha et al. [27] have reported that the higher the charge density of the cations, the more the hydrophilicity of the zeolite. Thus, one can conclude that the preparation method, the nature of cations as well as their concentration in zeolite structure could have great influences on the physical and chemical properties of the zeolite catalyst to consequently affect its sonocatalytic behavior.

#### X. CONCLUSION

Comparative study between titania encapsulated into internal pores of zeolite Y or being loaded on its external surface by changing the preparation method was performed to provide information on the differences in characteristics of the catalyst materials obtained and the subsequent catalytic performance under ultrasonic irradiation. The position and the amount of TiO<sub>2</sub> loaded into the zeolite were significantly influenced by the preparation method. Correlations between the preparation method and characteristics of the catalysts were successfully made. The crystallinity of zeolite remained unchanged after the encapsulation of TiO<sub>2</sub>. However, for the case of TiO<sub>2</sub> loading on the external surface of the zeolite using impregnation method, a wide peak of rutile phase was observed and the crystallinity of the zeolite significantly disappeared. The disappearance of the zeolite crystallinity was ascribed to the accumulation of TiO<sub>2</sub> on the surface of the support in addition to the amorphous nature of the titania precursor. SEM and TEM techniques provided evidences that the structure of zeolite was not significantly destroyed after the loading of TiO<sub>2</sub>. The decolorization of amaranth dye was 50 % and 68 % for titanium encapsulated zeolite (Ti<sub>4</sub>-NaY) and titanium impregnated on zeolite (15% TiO<sub>2</sub>-NaY) catalyst, respectively. The difference in the preparation method significantly affected the amount of TiO<sub>2</sub> loaded into the zeolite to subsequently affect the <sup>•</sup>OH radicals generation during the reaction. Furthermore, ultrasonic wave could more easily irradiate the TiO<sub>2</sub> clusters anchored on the external surface of the zeolite. Thus, the location of TiO<sub>2</sub> in the catalyst was more influential on the sonocatalytic activity.

#### REFERENCES

- [1] J. Wang, J. Li, Y. Xie, C. Li, G. Han, L. Zhang, R. Xu, X. Zhang, "Investigation on solar photocatalytic degradation of various dyes in the presence of Er<sup>3+</sup>:Y AlO<sub>3</sub>/ZnO-TiO<sub>2</sub> composite", *J. Environ. Manage.*, vol. 91, pp. 677-684, 2010.
- [2] A.N. Ökte, O. Yilmaz, "La and Ce loaded TiO<sub>2</sub>-ZSM-5 catalysts: Comparative characterization and photocatalytic activity investigations", *Micropor. Mesopor. Mat.* vol. 126 pp. 245-252, 2009.
- [3] J. Marugán, J. Aguado, W. Gernjak, S. Malato, "Solar photocatalytic degradation of dichloroacetic acid with silica-supported titania at pilot-plant scale", *Catal. Today.*, vol. 129, pp. 59-68, 2007.
- [4] Y. Zhang, S. Deng, B. Sun, H. Xiao, L. Li, G. Yang, Q. Hui, J. Wu, J. Zheng, "Preparation of TiO<sub>2</sub>-loaded activated carbon fiber hybrids and application in a pulsed discharge reactor for decomposition of methyl orange", *J. Colloid Interface Sci.*, vol. 347, pp. 260-266, 2010.
- [5] H. Yoneyama, S. Haga, S. Yamanaka, "Photocatalytic activities of microcrystalline TiO<sub>2</sub> incorporated in sheet silicates of clay", *J. Phys. Chem.*, vol. 93 pp. 4833-4837, 1989.
- [6] D.I. Petkowicz, R. Brambilla, C. Radtke, C.D.S. da Silva, Z.N. da Rocha, S.B.C. Pergher, J.H.Z. dos Santos, "Photodegradation of methylene blue by in situ generated titania supported on a NaA zeolite", *Appl. Catal. A: Gen.*, vol. 357, pp. 125-134, 2009.
- [7] X. Liu, K.-K. Iu, J. Kerry Thomas, "Encapsulation of TiO<sub>2</sub> in zeolite Y", *Chem. Phys. Lett.*, vol. 195, pp. 163-168, 1992.
- [8] A.N. Ökte, Ö. Yilmaz, "Characteristics of lanthanum loaded TiO<sub>2</sub>-ZSM-5 photocatalysts: Decolorization and degradation processes of methyl orange", *Appl. Catal. A: Gen.*, vol. 354, pp. 132-142, 2009.
- [9] H. Chen, A. Matsumoto, N. Nishimiya, K. Tsutsumi, "Preparation and characterization of TiO<sub>2</sub> incorporated Y-zeolite", *Colloid. Surf. A.*, vol. 157, pp. 295-305, 1999.
- [10] A. Corma, H. Garcia, "Zeolite-based photocatalysts", *Chem. Commun.*, vol. 10, pp. 1443-1459, 2004.
- [11] Y.L. Pang, S. Bhatia, A.Z. Abdullah, "Process behavior of TiO<sub>2</sub> nanotube-enhanced sonocatalytic degradation of Rhodamine B in aqueous solution", *Sep. Purif. Technol.*, vol. 77, pp. 331-338, 2011.
- [12] B. Cekova, D. Kocov, E. Kolcakovska, D. Stojanova, "Zeolites as alcohol adsorbents from aqueous solutions", *Acta Periodica Technol.*, pp. 83-87, 2006.
- [13] R.J. Tayade, R.G. Kulkarni, R.V. Jasra, "Enhanced photocatalytic activity of TiO<sub>2</sub>-coated NaY and HY zeolites for the degradation of methylene blue in water", *Ind. Eng. Chem. Res.*, vol. 46, pp. 369-376, 2007.
- [14] E.P. Reddy, L. Davydov, P. Smirniotis, "TiO<sub>2</sub>-loaded zeolites and mesoporous materials in the sonophotocatalytic decomposition of aqueous organic pollutants: the role of the support", *Appl. Catal. B: Environ.*, vol. 42, pp. 1-11, 2003.
- [15] A.Z. Abdullah, P.Y. Ling, "Heat treatment effects on the characteristics and sonocatalytic performance of TiO<sub>2</sub> in the degradation of organic dyes in aqueous solution", *J. Hazard. Mater.*, vol. 173, pp. 159-167, 2010.
- [16] C.C. Wang, C.K. Lee, M.D. Lyu, L.C. Juang, "Photocatalytic degradation of C.I. Basic Violet 10 using TiO<sub>2</sub> catalysts supported by Y zeolite: An investigation of the effects of operational parameters", *Dyes Pigments.*, vol. 76, pp. 817-824, 2008.
- [17] V. Durgakumari, M. Subrahmanyam, K.V. Subba Rao, A. Ratnamala, M. Noorjahan, K. Tanaka, "An easy and efficient use of TiO<sub>2</sub> supported HZSM-5 and TiO<sub>2</sub>+HZSM-5 zeolite combine in the photodegradation of aqueous phenol and p-chlorophenol", *Appl. Catal. A: Gen.*, vol. 234, pp. 155-165, 2002.
- [18] S.H. Bossmann, C. Turro, C. Schnabel, M.R. Pokhrel, L.M. Payawan Jr, B. Baumeister, M. Wörner, "Ru (bpy)<sub>3</sub><sup>2+</sup>/TiO<sub>2</sub>-codoped zeolites: synthesis, characterization, and the role of TiO<sub>2</sub> in electron transfer photocatalysis", *J. Physic. Chem. B.*, vol. 105, pp. 5374-5382, 2001.
- [19] S. Easwaramoorthi, P. Natarajan, "Photophysical properties of phenosafranine (PHNS) adsorbed on the TiO<sub>2</sub>-incorporated zeolite-Y", *Micropor. Mesopor. Mat.*, vol. 86, pp. 185-190, 2005.
- [20] G.P. Joshi, N.S. Saxena, T.P. Sharma, S.C.K. Mishra, "Measurement of thermal transport and optical properties of conducting polyaniline", *Indian J. Pure Appl. Phys.*, vol. 44 pp. 786-790, 2006.
- [21] M. Anpo, H. Yamashita, M. Matsuoka, P. Dal-Ryung, S. Yong-Gun, P. Sang-Eon, "Design and development of titanium and vanadium oxide photocatalysts incorporated within zeolite cavities and their



photocatalytic reactivities”, *J. Ind. Eng. Chem. Seoul.*, vol. 6, pp. 69-71, 2000.

- [22] H. Hassan, B.H. Hameed, “Oxidative decolorization of Acid Red 1 solutions by Fe-zeolite Y type catalyst”, *Desalination.*, vol. 276, pp. 45-52, 2011.
- [23] S. Yamaguchi, T. Fukura, Y. Imai, H. Yamaura, H. Yahiro, “Photocatalytic activities for partial oxidation of  $\alpha$ -methylstyrene over zeolite-supported titanium dioxide and the influence of water addition to reaction solvent”, *Electrochim. Acta.*, vol. 55, pp. 7745-7750, 2010.
- [24] S. Easwaramoorthi, P. Natarajan, “Characterisation and spectral properties of surface adsorbed phenosafranine dye in zeolite-Y and ZSM-5: Photosensitisation of embedded nanoparticles of titanium dioxide”, *Micropor. Mesopor. Mat.*, vol. 117, pp. 541-550, 2009.
- [25] W. Zhang, L. Zou, L. Wang, “Photocatalytic TiO<sub>2</sub> adsorbent nanocomposites prepared via wet chemical impregnation for wastewater treatment: A review”, *Appl. Catal. A: Gen.*, vol. 371, pp. 1-9, 2009.
- [26] A. Pourahmad, S. Sohrabnezhad, “A cost effective and sensitive method for the determination of ammonia concentration in nanocrystal mordenite”, *Int. J. Nano. Dim.*, vol. 1, pp. 143-152, 2010.
- [27] F. Serralha, J. Lopes, F. Lemos, D. Prazeres, M. Aires-Barros, J. Cabral, F. Ramoa Ribeiro, “Zeolites as supports for an enzymatic alcoholysis reaction”, *J. Mol. Catal. B: Enzym.*, vol. 4, pp. 303-311, 1998.